Production of Neutral Mesons by 340-Mev Protons on Hydrogen

J. W. MATHER AND E. A. MARTINELLI
Radiation Laboratory, Department of Physics, University of California, Berkeley, California
(Received April 15, 1953)

The production of neutral mesons by 340-Mev protons on hydrogen has been measured directly by detecting a single gamma ray from the two gamma-ray decay of a neutral meson, at 90° to the proton beam. A liquid hydrogen target and a focusing Čerenkov counter are described. The ratio of the cross section for neutral meson production from hydrogen relative to carbon is

$$\sigma_H/\sigma_C=0.0059\pm0.0009,$$

where the error is standard deviation. Using the absolute cross section of neutral meson production from carbon as 1.5×10^{-27} cm², one obtains the neutral meson production cross section for hydrogen to be 8.8×10^{-30} cm².

The transition $^3P\rightarrow{}^1S$ (allowed by the conservation of angular momentum and parity) for the protons can be interpreted as a triplet p-state interaction with emission of an s-state neutral meson. The agreement with the existing data at proton energies of 440 Mev is fair. The 340- and 440-Mev data give two points on the neutral meson excitation function curve, showing a steep rise. The experimental results give some evidence for the breakdown of the approximate selection rule which forbids the emission of s-state neutral mesons with final s-state nucleons. The relative cross section for carbon and nitrogen indicates that the yield of neutral mesons is due to the interaction of the incident protons with the neutrons in the nuclei.

INTRODUCTION

IT has been established by Hales, Hildebrand, Knable, and Moyer[1] using a CH_2-C subtraction method, that the production cross section of neutral mesons by 340-Mev protons on hydrogen is either zero or less than two percent of the carbon yield. An attempt was made to measure the direct production of neutral mesons from a liquid hydrogen target at 90° to the 340-Mev proton beam, using a Čerenkov radiation counter[2,3] that employs a triple coincidence technique to view the Čerenkov radiation. At the beginning of the experiment, it was thought that the experimental result would yield at least an upper limit for neutral meson production from hydrogen because only one gamma ray from a two gamma-ray neutral meson decay[4,5] was detected. No attempt was made to detect the coincident gamma rays from neutral meson decay, because of the expected low yield.

TABLE I. Transitions allowed by Pauli principle, conservation of angular momentum and parity for production of pseudoscalar neutral mesons in nucleon-nucleon collisions $(p, p\pi^0)$.

Initial state p, p	Final state π^0 meson	p, p	Transition
$^1S_0$	s	$^3P_0$	$^1S_0\rightarrow{}^3P_0$
	p	forbidden	none
$^3P_0$	s	$^1S_0$	$^3P_0\rightarrow{}^1S_0$
↓	p	$^3P_1$	$^3P_0\rightarrow{}^3P_1$
etc.			

Recent evidence of the hydrogen cross section at bombarding proton energies of 440 Mev has been obtained by Marshall, Marshall, Nedzel, and Warshaw,[6] showing that the production cross section of neutral mesons from hydrogen is $0.45\pm0.15\times10^{-27}$ cm² at that energy.

For the reaction $(p, p\pi^0)$, assuming a pseudoscalar neutral meson emitted in a p state, and if only s states for the product nucleons are considered, it can be shown from the conservation laws of total angular momentum and parity that the above reaction is forbidden. If the production of mesons in p states represents a universal type of coupling for nucleon-nucleon collisons, then there exists a general selection rule prohibiting the $(p, p\pi^0)$ process for final s-state nucleons.

From an examination of Table I, transitions yielding higher angular momentum states for the two final protons are possible, but since the energy available to the two final protons in the center-of-mass system is approximately 8 Mev, higher angular momentum states than s states will be suppressed. However, the transition $^3P\rightarrow{}^1S$ yielding an s-state meson is possible and is thought to be responsible for the neutral mesons observed near the threshold.

There is evidence from the $(p, p\pi^+)$ experiment by Cartwright, Richman, Wilcox, and Whitehead[7] and more recently by Schulz[8] that the positive pi meson is emitted predominately in a p state in the center-of-mass system. However, the s-state yield of positive mesons is not zero[8] and is thought to be approximately one-eight to one-tenth of the p-state yield.

[1] Hales, Hildebrand, Knable, and Moyer, Phys. Rev. **85**, 373 (1952).
[2] J. Marshall, Phys. Rev. **81**, 275 (1951).
[3] J. W. Mather and E. A. Martinelli, University of California Radiation Laboratory Report UCRL-1646, 1952 (unpublished).
[4] Steinberger, Panofsky, and Steller, Phys. Rev. **78**, 802 (1950).
[5] C. N. Yang, Phys. Rev. **77**, 242 (1950).
[6] Marshall, Marshall, Nedzel, and Warshaw, Phys. Rev. **88**, 632 (1952).
[7] Cartwright, Richman, Wilcox, and Whitehead, Phys. Rev. **78**, 823 (1950) and **81**, 652 (1951).
[8] A. G. Schulz, Jr., Ph.D. Thesis, University of California Radiation Laboratory Report UCRL-1756, 1952 (unpublished).

Even though the pi meson is emitted primarily in a p state with respect to the nucleon, it can nevertheless be shown qualitatively that there exists some s-state meson emission with respect to the center of mass of the two proton system. For example, if for distances close to the nucleon the meson wave function for p-state emission is given as $\psi \sim kr$, where k is the meson momentum in the center of mass, and r the relative distance from the nucleon, then ψ can be transformed to $\psi' \sim k(r_0 \cos\theta + R)$, where r_0 can be taken as half the range of nuclear forces in p-p collisions, and R is the distance relative to the center of mass of the two nucleon system. In evaluating the matrix element, however, the p-state term vanishes because of the selection rule; the cross term vanishes due to the orthogonality of the s and p waves, leaving only the s-state term.

Hence the quantity $(r_0/\lambda\!\!\!^{-})^2$ can be interpreted as the fraction of mesons that are emitted in p states with respect to the nucleon, but in s states with respect to the center of mass of the two nucleon system. The above discussion holds only for the case where $r_0 < \lambda\!\!\!^{-}$. As the energy increases, r_0 may become large compared to $\lambda\!\!\!^{-}$, and the estimate breaks down because the wave functions are no longer valid for large R. Thus it may be said that in the $^3P \rightarrow {}^1S$ transition, the meson is emitted from a p state with respect to either nucleon, but comes out in an s state with respect to the center of mass of the two nucleon system, leaving the product nucleons in s states.

EXPERIMENTAL ARRANGEMENT

The general plan view of the 184-inch synchrocyclotron is shown in Fig. 1(a). The 340-Mev proton beam was initially collimated by a premagnet collinating slit system before it was bent by the steering magnet so as to enter a two-inch diameter, 48-inch long brass collimator extending through the concrete shielding surrounding the cyclotron. Most of the beam shaping is achieved at the premagnet slits to prevent the spray of neutrons and general radiation from entering the detection area.

The scattered beam has approximately a 20-microsecond duration with a repetition rate of 50 cycles per second. This yields a duty cycle of 10^{-3} defined as the fraction of time the beam is on. The flux of protons in the scattered beam for this experiment was maintained at approximately 5×10^8 protons per second, and was continuously monitored by a CO_2-argon filled ionization chamber which was connected to an electrometer in the counting area. The electrometer actuated a Speedomax recorder which gave a visual indication of the proton beam level at all times.

The general arrangement of the liquid hydrogen flask, magnet and Čerenkov counter is shown in Fig. 1(b). The physical size of the water-cooled magnet determined both the position of the hydrogen target relative to the proton beam snout and also the location of the Čerenkov counter with respect to the hydrogen target. With this geometry, the counting rate will vary inversely as the distance from the target, because the effective target thickness varies as the distance from the target to the detector, while the solid angle subtended by the detector at the target varies inversely as the distance squared. The water cooled magnet served to sweep the $\frac{3}{4}$-inch diameter channel free of charged particles which would have given an erroneous hydrogen counting rate. Sources of background are discussed in a later section.

Since the neutral meson counting rate was expected to be not more than 1 percent of the carbon yield, it

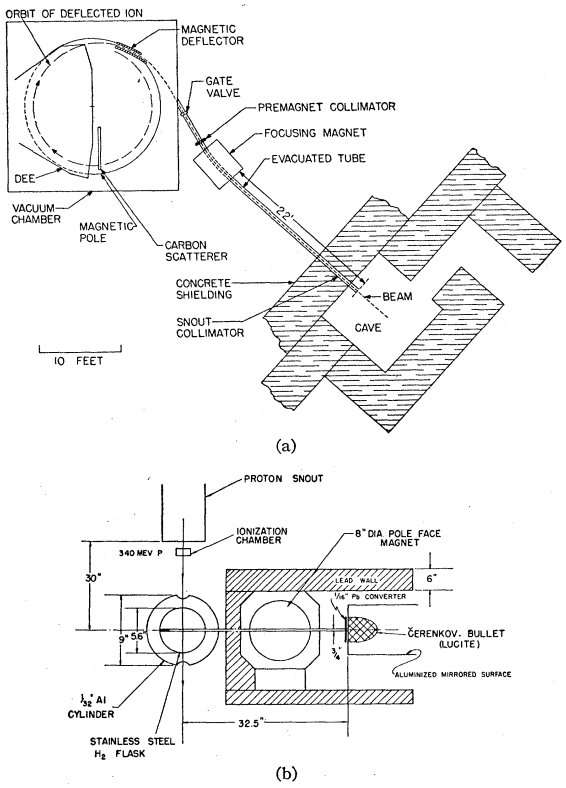

FIG. 1(a) Cyclotron layout. (b) Experimental arrangement in the cave, showing relative positions of hydrogen target, magnet, and Čerenkov counter.

was desirable that the background rate be at least an order of magnitude lower. Even though we employed a focusing type Čerenkov radiation counter, it was to our advantage to set up at 90° to the proton beam to obtain adequate shielding of the photomultipliers. The amount of shielding required was determined during previous cyclotron runs, and also the possibility of setting up at angles other than 90° were investigated.

ČERENKOV COUNTER

The theory of Čerenkov radiation as developed by Frank and Tamm,[9] leads to the equation $\cos\theta = c/\eta v$,

[9] I. Frank and I. Tamm, J. Phys. (U.S.S.R.) **1**, 439 (1939).

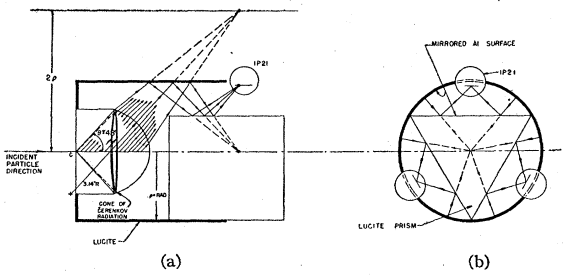

FIG. 2. Detail of Čerenkov counter. (a) Side view of triples detection scheme showing only 1 tube. (b) End view showing placement of three 1P21 photomultipliers.

where θ is the half-angle of the Čerenkov radiation cone, η is the index of refraction of the medium, v is the velocity of the charged particle in the medium, and c the velocity of light in vacuum. For a very fast electron ($v \approx c$) passing through Lucite ($\eta = 1.5$), the number of quanta emitted in the 1P21 photomultiplier spectral region per centimeter of path is approximately 425 quanta per centimeter.

The design of the Čerenkov counter is similar to Marshall's, except that a triple coincidence photomultiplier arrangement is employed to view the Čerenkov radiation. Figure 2 shows the general view of the counter. Gamma rays from the neutral meson decay are converted to fast electrons in a thin lead plate placed before the Lucite radiator [Fig. 1(b)].

Before we discuss the performance of the Čerenkov counter, a brief account of the general problem of focusing of Čerenkov radiation should be mentioned. The Lucite radiator is a partial spherical surface of radius 3.14 inches and neglecting any dispersion in angle, the cone of radiation will be focused into a ring twice the radius of curvature as measured from the vertex of the spherical surface. A cylindrical aluminized mirror of half the ring diameter intercepts the Čerenkov rays and reflects them to a focal spot on the central axis, assuming that the initial particles enter the Lucite radiator along the central axis. An aluminized prism is so placed to intercept these rays and focus them onto the cathodes of the photomultipliers (Fig. 3). Each particular particle direction in the Lucite generates its own cone of radiation, and if the Čerenkov rays are geometrically followed through the optical system it is then clear that each cone of radiation will be focused at a place determined by the original particle direction. In particular, neglecting spreading of the Čerenkov cone, the radiation from an on-axis particle will be focused at a point on the central axis because the cone originated on the axis. However, for off-axis origin of the Čerenkov cone, a large fraction of the Čerenkov rays will never intersect the axis and, consequently, will come to a focus off the central axis. Thus, one can expect a general region of focal points at the detector from all the photons that make up the initial cone of radiation.

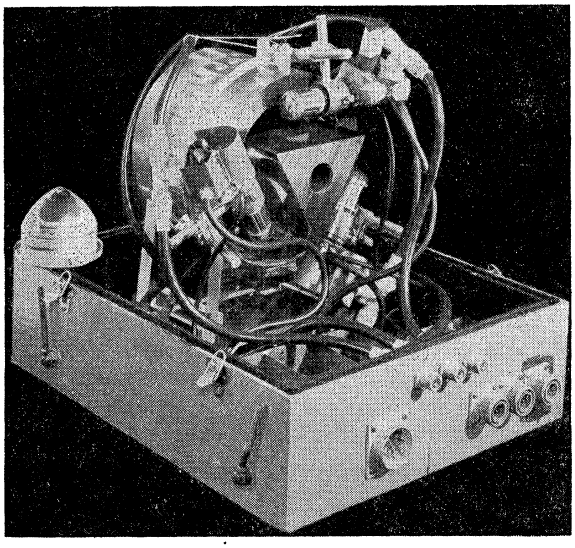

FIG. 3. Photograph of Čerenkov counter.

Initially a double coincidence arrangement[3] was constructed, using only two photomultipliers as detectors. This design was subjected to experiment to determine the effective aperture, directional properties, and, if possible, an efficiency for detecting gamma rays. It was determined, prior to experiment, that off-axis particles would not be counted as effectively as on-axis particles, and furthermore, particles entering the Lucite radiator making a large angle with the central axis would not be effectively counted. These effects can be approximated, but the analysis is complicated by the small multiple angle Coulomb scattering occurring in the radiator, and since Čerenkov radiation contains a mixture of wavelengths extending over the entire visible spectrum, one can expect a small amount of dispersion in Lucite. Dispersion, therefore, will will spread the Čerenkov cone of radiation in angle. The foregoing effects, combined with the problem of focusing the Čerenkov radiation cone, make it necessary to use positioning devices for the photomultipliers. Other designs of Čerenkov counters (Marshall[10] gives a complete account of various designs) have been used successfully. Lucite material was chosen for the Čerenkov radiator because of (1) the ease of machining and polishing to the desired form, (2) the low atomic number, approximately 7, leading to small multiple angle Coulomb scattering, and (3) the low density and atomic number resulting in a small rate of energy loss through ionization for a charged particle traversing the Lucite.

The performance of a two-photomultiplier Čerenkov counter[3] was determined, using the 320-Mev Berkeley synchrotron. The x-ray beam was collimated to $\frac{1}{8}$-inch diameter and allowed to impinge on a thin lead converter placed before the Lucite radiator. By careful

[10] J. Marshall, Phys. Rev. 86, 685 (1952).

alignment of the axis of the Čerenkov radiator with the direction of the x-ray beam, it was possible to obtain the curves shown in Figs. 4 and 5 giving the aperture width at half maximum of 0.6-inch and the angular acceptance at half maximum of approximately 2.5°, respectively. Prior to this, data were obtained giving the response of the Čerenkov counter as a function of the photomultiplier position on the metal ring. The positioning devices were adjustable in all directions, and maximum counting rate was obtained approximately at the predicted angle for fast electrons, with the Čerenkov rays coming to a focus at the sensitive cathode surface. The velocity selection was checked by moving one photomultiplier one cathode-width off the determined position; the counting rate dropped a factor of 7. A further check to test the Čerenkov effect was made by reversing the counter 180°, allowing the electrons to impinge on the back of the Lucite radiator. No counts were obtained that were statistically significant from pure accidentals as determined from a known length of delay cable placed in one leg of the coincidence circuit.

At the 184-inch cyclotron, it was possible to obtain a figure for the efficiency of detecting gamma rays with energies in the range of 40–120 Mev by using the gamma-ray decay of the neutral meson. The neutral mesons were produced by the 340-Mev circulating proton beam incident on a $\frac{1}{4}$-inch carbon target at point "*a*" shown in Fig. 1(a). The decay gamma rays were observed through the neutron hole in the concrete shielding in the zero degree direction approximately 50 feet from the internal carbon target. Since previous experiments on neutral mesons from carbon were performed by Crandall[11] using the pair spectrometer, it was felt that the efficiency of the Čerenkov counter, based on the gamma-ray yield as recorded by the spectrometer, would be a reliable figure. The ratio of observed coincidences to the total number of gamma rays incident on the Lucite radiator (effective aperture approximately 0.6 inch in diameter was as high as 21 percent). This efficiency is not to be construed to mean that a coincidence plateau was obtained, but rather indicates a result for a given voltage and discriminator setting.

If the effect of spreading in angle of the Čerenkov cone is considered along with the foregoing discussion of off- and on-axis particles, then it is clear that the curves shown in Figs. 4 and 5 are indicative that Čerenkov radiation was being detected and not general fluorescence. One would not expect fluorescence in Lucite, if present, to exhibit the directional property as shown.

In conclusion, the curves shown in Figs. 4 and 5 indicate (1) this particular design of counter has the advantage of being directional; (2) the Lucite radiator has no definite sensitive detection area; (3) even though the half-maximum width be taken as the effective area, the resulting solid angle is extremely small; (4) the efficiency of detection of off-axis particle is falling extremely rapidly; and (5) the effective aperture of the Lucite radiator at half-maximum is reasonably close to the combined widths of the photocathode surfaces (approximately 2 centimeters) as expected.

Whenever high-energy gamma rays are detected, it is important to determine whether a converter effect is

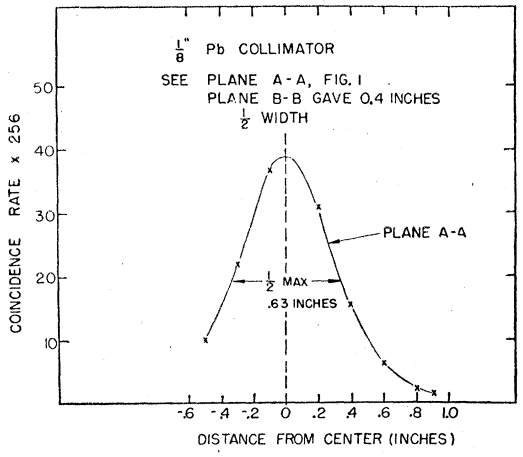

FIG. 4. Variation of response across diameter of Lucite radiator.

obtained. For the Čerenkov counter, this was carried out by placing thin sheets of lead before the Lucite radiator and observing the coincidence rate as a function of the thickness of the converter. This procedure was

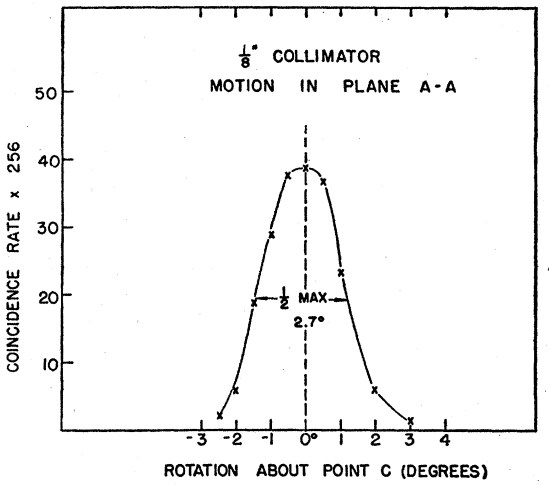

FIG. 5. Variation of response under rotation of counter about point *C*.

also used for the double scheme, yielding similar results. Considering only the lead converter, although copper curves (Fig. 6) were also obtained. characteristic curves were obtained for the attenuation part of the curve, but the transition from no lead to the peak of the transition curve was, at most, a factor of 2–3 at a

[11] W. Crandall, Ph.D. thesis, University of California Radiation Laboratory Report UCRL-1637, 1952 (unpublished).

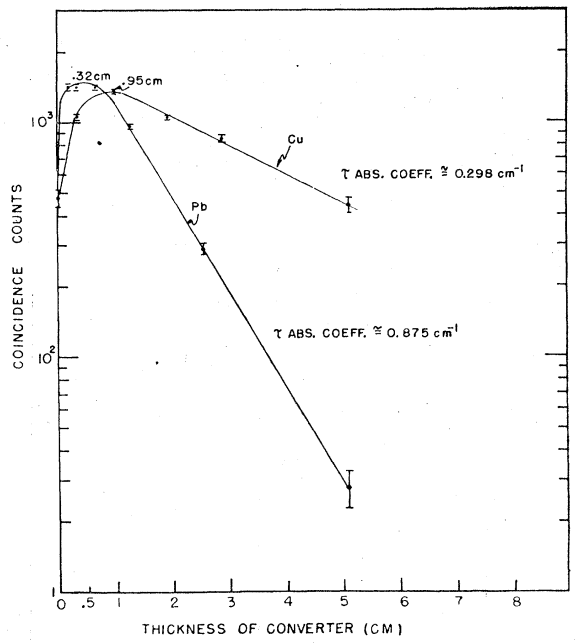

FIG. 6. Attenuation curves for the neutral meson decay gamma rays in lead and copper. The data were taken with a Čerenkov counter directed at a $\frac{1}{4}$-inch internal carbon target in the 340-Mev circulating proton beam.

converter depth of $\frac{1}{16}$- to $\frac{1}{8}$-inch lead. The directional properties of the counter have already been discussed; hence, it is not unreasonable to expect the small multiple angle scattering in lead and Lucite to cancel the effects of the increased pair production in lead. Some evidence for this is given by the lead and copper transition curves in Fig. 6, showing that the same maximum counting rate is obtained for each converter materials.

ELECTRONICS

A block diagram of the electrical arrangement is shown in Fig. 7. The general sequence is clear; each photomultiplier pulse is limited, clipped, and amplified before a coincidence is made. However, two separate coincidence circuits were employed. Pulses 1 and 2 (Fig. 7) are placed in coincidence, using one 6BN6 (minature beam tube). The output of this coincidence is further placed in coincidence with a properly delayed third photomultiplier signal. The resolving time obtained with this arrangement is approximately 10^{-8} second. The triple coincidence output is then amplified and scaled in the conventional manner.

A few remarks should be made concerning the components of the electrical system, for it may seem that more effective circuitry should have been used. The limiter circuit (not shown) employs a sharp cutoff pentode 6AH6, mounted at the base of a 1P21 photomultiplier (Fig. 3) to avoid long signal leads which would increase the capacitance to ground and thereby decrease the high frequency response of the circuit. To avoid using more than one distributed amplifier per photomultiplier, a large grid resistance of approximately 9K is placed in the grid circuit of the 6AH6. The voltage developed across the grid resistance is ample for limiting action. However, it is to be remarked that the dead time of the circuit seriously limits fast counting. Fast counting in this particular experiment is of no importance; however, we were concerned with the thermal noise rate of the photomultiplier jamming the limiter circuit. By selecting good photomultipliers with a low noise component, we operated well below the allowed repetition rate. The use of this circuit required only one amplifier per photomultiplier and thus avoided complex electronic setup and maintenance.

The triple coincidence circuit (Fig 8), employing the miniature beam tube 6BN6, has the advantage of simplicity of design. Resolving times of approximately 10^{-10} second have been reported using square pulses, while resolving times of approximately 5×10^{-9} second have been obtained using photomultiplier pulses. The tube normally operates completely cut off, requiring positive pulses on both grids for coincidence. However, the control grid nearest the plate, being unshielded from the plate circuit, allows grid pulses to capacity feed-through to the plate. The feed-through problem is particularly important when a slight negative overshoot is present on the signal pulse, as is the usual case with amplified pulses. It is seen that the negative part of the impressed signal will capacity-couple to the plate, giving rise to a pulse of the same polarity as the real coincidence pulse. By increasing the plate load resistance, the feed-through pulse height can be made negligible compared to the coincidence pulse. However, one does not gain pulse height selection without losing in another respect. If the coincidence pulse is to be used in coincidence with a third signal as is done in this experiment, one must be concerned with the RC time constant of the grid plate circuit. Attempts were made to keep the time constant to approximately 10^{-8} second. However, if the coincidence pulse is to be scaled directly, then the broadening of the coincidence pulse matters little. In any event, this broadening is not a serious objection, but one must be cognizant of its presence in this particular tube. Another remark should be made concerning the time delay between the signals applied to both grids.

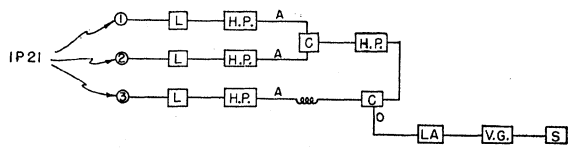

FIG. 7. Block diagram of electronics. L=limiter (6AH6); H,P=distributed amplifier (100 Mc/sec); LA=linear amplifier (10 Mc/sec); C=6BN6, coincidence $\tau\sim10^{-8}$ sec; $V.G.$=variable gate; S=scaler.

The grid nearest the plate should be delayed approximately 2×10^{-9} second for resolving times of this order. However, this is a small correction for resolving times of 10^{-8} second.

The grid bias for the 6BN6 can be controlled separately by negative bias, or both grids can be controlled simultaneously by the cathode bias. The authors have tried both methods of control, with the result that separate control is more flexible for Čerenkov signals. It is further known that all the light pulses from Čerenkov radiation are not limited, and further, that the gain of the wide band amplifiers were not the same. It was for this reason that we found separate grid control advantageous.

The coincidence circuit (Fig. 9) was used in the double photomultiplier scheme referred to in the previous section. This circuit follows closely that outlined by Bay[12] but was further developed by Neher.[13] The balanced bridge circuit is well understood; however,

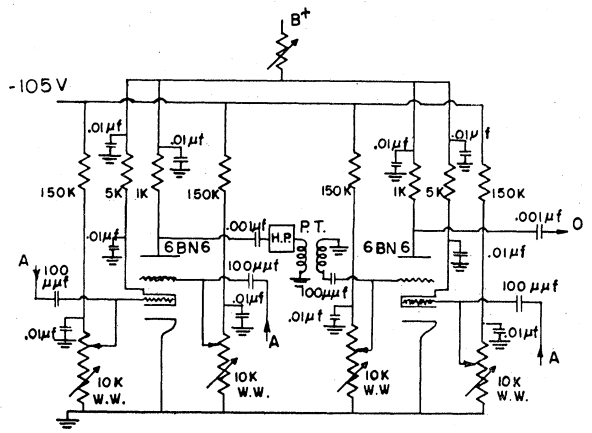

FIG. 8. Triple coincidence network. *A*—positive signal in; *O*—positive signal out (see Fig. 9). *P.T.*—pulse transformer. $\tau\sim10^{-8}$ sec.

for successful operation the crystal diodes should have a high-backward to low-forward resistance. The unbalance at the midpoint of the bridge by two positive signals is then detected by a difference amplifier. It is known that this coincidence circuit is strongly pulse-height dependent, and for this reason, and also to avoid the complexity of a triple coincidence bridge network, the circuit in Fig. 8 was developed.

LIQUID HYDROGEN TARGET

The problem of converting an in-line liquid target[14] to an approximate point source was carried out by Garrison.[15] The in-line target superstructure, however, was carried over to the new design without change. A cross-sectional view of the target is shown in Fig. 10.

[12] Z. Bay, Rev. Sci. Instr. **21**, 297 (1951).
[13] L. Neher (private communication).
[14] L. Cook, Rev. Sci. Instr. **22**, 1006 (1951).
[15] J. Garrison (private communication).

Since the Čerenkov counter detects only gamma rays from the hydrogen target, local sources of gamma rays had to be considered, and these are discussed in the next section. Fortunately, the important source of background gammas originated in a second-order process, and were effectively reduced by requiring that the wall thickness of the liquid hydrogen container be as thin as possible. It was felt that a 2-mil stainless steel foil would be sufficient for mechanical strength, but the quality of the available stainless steel foil was poor. As a result, the liquid flask was fabricated from a 4-mil stainless steel foil in the form of a cylinder 5.6 inches in diameter and 8 inches in length. The foil was soft-soldered to a stainless steel base and to a collar arrangement on the vertical hydrogen tube. To prevent appreciable loss of liquid hydrogen by conduction up the vertical hydrogen tube, a liquid nitrogen jacket was used. The outside aluminum jacket surrounding the hydrogen flask was 9 inches in diameter with $\frac{1}{16}$-inch wall thickness, except where the proton beam penetrated. At this point there was a 3-inch diameter hole, covered with a 5-mil aluminum foil to reduce negative meson production. Since the proton beam emerges from a 2-inch diameter collimator [Fig. 1(a)], there is sufficient tolerance in the 3-inch diameter hole so that no protons impinge on the thick-walled aluminum jacket. Frequent photographs of the beam alignment were made throughout the experiment.

A test (using liquid nitrogen in place of liquid hydrogen) was performed to determine whether any gas bubbles were present in the liquid nitrogen. When the liquid nitrogen reached a quiescent state, it was possible to look down the hydrogen tube and observe the liquid surface. This was checked several times and no bubbles were observed. Therefore it was assumed that liquid hydrogen would not bubble to any great extent because the temperature difference between liquid nitrogen and hydrogen is only 50°. A further

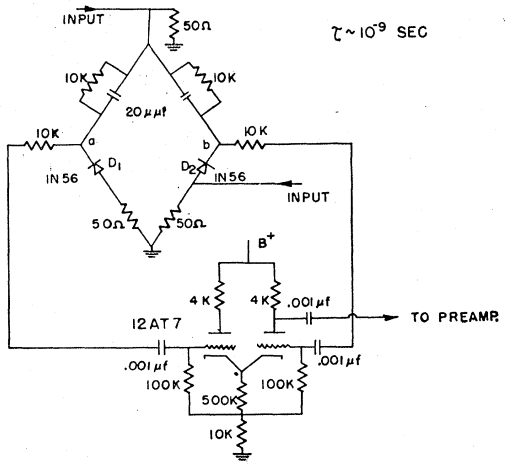

FIG. 9. Crystal diode coincidence circuit and difference amplifier.

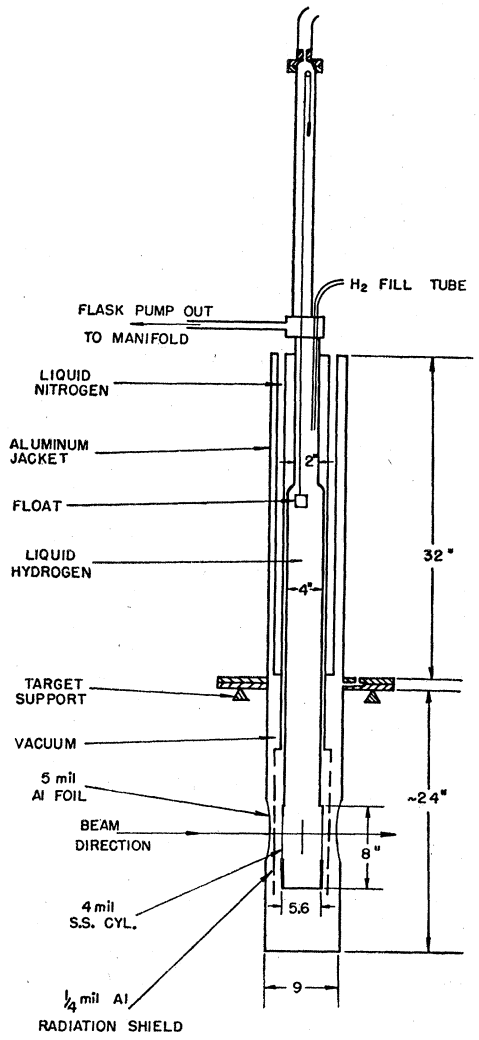

FIG. 10. Detail of liquid hydrogen target.

check of all heat losses was obtained during the hydrogen experiment over a period of twenty-four hours; it was found that the disappearance of liquid hydrogen corresponded to a heat flow of approximately 0.2 calories sec^{-1}. Since the hydrogen was continually vented to the atmosphere through a 2-inch diameter rubber hose, it is not difficult to account for most of the heat loss in this way. Thus, it was concluded that no boiling of the liquid hydrogen in the sensitive volume of the proton beam was present.

No provision was made for filling and emptying the hydrogen target during the experiment. However, the hydrogen target assembly provided a blank target, identical to the hydrogen target, except that it was not evacuated. The blank target and the liquid hydrogen target were fixed in place on a movable carriage, facilitating a change in target in a matter of minutes. Because of the orientation of the target frame relative to the proton beam, it was necessary to remove the dummy target each time the liquid hydrogen target was used.

SOURCES OF BACKGROUND

Before considering the kind of background that could conceivably lead to an erroneous interpretation of the hydrogen result, it might be well to indicate the magnitude of the expected yield of neutral mesons from protons bombarding hydrogen. Taking the hydrogen yield of neutral mesons to be approximately one percent of the carbon yield[16] as indicated by Hales *et al.*, then the gamma-ray intensity[17] at the target can be expressed as

$$N(\gamma)=0.52\times10^{-29}N_0F_P,$$

where N_0 and F_P are Avogadro's number and proton flux, respectively. However when the efficiency and solid angle factors are included, the expected rate is of the order of one count per 15 minutes. It was therefore obvious at the beginning that the background counting rate must be made at least an order of magnitude lower; otherwise cyclotron running time would be prohibitively long to obtain reasonable counting statistics. The experiment was undertaken, using a Čerenkov focusing detector previously described which had demonstrated its ability to select only those particles which enter the Lucite radiator making a small angle with the normal to the radiator of approximately 1.5°.

Besides maintaining the accidental rate due to photomultiplier tube noise to a negligible value, the following possible sources of background were considered:

(1) π^+ production in hydrogen and its associated μ-e electron decay;
(2) fast electrons from targets;
(3) π^-, π^+ ordinary scattering in hydrogen at 90°;
(4) π^- charge exchange in hydrogen;
(5) π^0 production in the walls of the hydrogen container;
(6) π^- production in the window of the container, leading to capture in hydrogen.

All reactions involving the production or scattering of charged particles in hydrogen were mitigated by the use of a small magnet [Fig. 1(b)] capable of producing a magnetic field of approximately 20 000 gauss across a one-inch gap. The positive pi mesons produced in the reaction $(p, p\pi^+)$, fast electrons from nuclei bombarded by 340-Mev protons as found by Neher, Alvarez, and Moyer,[18] and the ordinary scattering of negative and positive mesons in hydrogen as

[16] The absolute cross section for neutral meson production from carbon is 1.5×10^{-27} cm² as measured by Crandall.
[17] The neutral meson decays into two gamma rays.
[18] Neher, Alvarez, and Moyer (private communication).

considered by Anderson,[19] and Fermi,[20] were bent out of the field of view of the Čerenkov detector.

Using the Fermi *et al.* data on the charge exchange of negative pi mesons[21] in hydrogen at 90°, and considering only the upper end of the negative pi spectrum for 340-Mev protons on carbon and lead, one obtains for the number of π^- mesons that will charge exchange in hydrogen at 90°:

$$N(\pi^-)=0.000065N_0F_P\times10^{-29}.$$

Clearly, this will give a negligible contribution of neutral mesons.

The directional properties of the Čerenkov counter made it possible to avoid π^0 contamination from the walls of the hydrogen container. The probability of a proton scattering to the far wall, as seen by the counter, and producing a π^0 meson is extremely small.

Reaction (6) was thought to be the only local source of significant background. Negative mesons produced by protons[22] on aluminum and the stainless steel foil surrounding the hydrogen can lead to capture in hydrogen giving rise to neutral mesons. With reference to Richman, Weissbluth, and Wilcox's[23] data, the low-energy π^- yield from aluminum and stainless steel windows was estimated, assuming that the negative meson production depends on the number of neutrons in the nucleus. The negative meson was chosen to stop in the sensitive portion of the target and thus be captured. Both the forward and backward production of negative mesons were considered, with the appropriate solid angle factor. If one combines the yield of negative mesons from 10-mils of aluminum and 8-mils of stainless steel, one obtains the number of gamma rays as a result of negative meson capture in hydrogen to be:

$$N(\gamma)=0.0124\times10^{-29}N_0F_P.$$

This estimation is based on a conservative analysis and therefore represents the bulk of the background. By inserting additional thicknesses of aluminum in front of the hydrogen container it is possible to test whether or not negative pi meson capture is important. A linear effect in counting rate should be observed if capture is taking place.

RESULTS

Since the experiment was expected to yield a low counting rate, the authors were constantly on guard to assure that all electronics equipment continued to perform in good order. To dispel any uncertainty, a carbon target approximately 1½ inches thick was placed in the proton beam periodically in place of the liquid target. Repeating this procedure after a blank- or liquid-target exposure gave full assurance of the operation of the coincidence circuit and Čerenkov counter throughout the 32-hour run. In addition, the carbon target offered a convenient source of neutral mesons, thus providing means of obtaining the proper coincidence pulse levels. The alignment of the Čerenkov counter and lead channel with the proton beam was rather critical because 90 percent of the protons emerging from the proton snout were concentrated in a line pattern approximately one-eighth inch wide, characteristic of the proton beam from the Berkeley synchrocyclotron.

After adjusting the electronic gear to count neutral mesons from carbon, the empty hydrogen target was bombarded for a period of two hours, with no measurable yield. The empty target was then filled with liquid hydrogen, and it remained filled through the entire experiment.

A further check on the possibility of observing neutral mesons from the far target wall [Fig. 1(b)] was made by comparing the coincidence rate of the blank target to that when no target was present. The yield in both cases was the same within statistics and was compatible with the neutral meson yield expected from air, based on the nitrogen and oxygen content of the air column in front of the Čerenkov counter. However, the statistics are poor but nevertheless significant. It is on this basis that no subtraction of the counts due to the air was made to the hydrogen result. At the end of the experiment, the liquid hydrogen was removed from the target and replaced by liquid nitrogen for the purpose of comparing the nitrogen results with carbon. The yield of neutral mesons from nitrogen was in good agreement with the carbon data and gave a further check on the consistency of operation of the electronic gear.

During one or two carbon target exposures, the accidental coincidence rate was checked by delaying[24] one leg of the coincidence circuit; no accidentals were measured, and on this basis none were expected from the liquid hydrogen target.

Because of the small sensitive volume of the target, compared to its dimensions [Fig. 1(b)], it was necessary to correct the experimental data for the attenuation of the proton beam through ionization and also for the decrease in intensity of the neutral meson decay gamma rays due to pair production in the target material.

Since the sensitive volume of each target as defined by the collimating system was at the center of the target in each case, it was necessary to consider the energy loss of a 340-Mev proton in passing through the insensitive part of the target. The insensitive portion

[19] Anderson, Fermi, Long, Martin, and Nagle, Phys. Rev. 85, 934 (1952).
[20] Fermi, Anderson, Lundy, Nagle, and Yodh, Phys. Rev. 85, 935 (1952).
[21] Positive mesons do not charge-exchange in hydrogen because of charge conservation.
[22] Negative mesons are not produced in hydrogen by protons because of charge conservation.
[23] Richman, Weissbluth, and Wilcox, Phys. Rev. 85, 161 (1952).
[24] Delay of approximately 6×10^{-8} second was used corresponding to the interval of time between two radio frequency pulses of the cyclotron.

of each target, i.e., 2.5 centimeters of carbon, 7 centimeters of liquid nitrogen, and 7 centimeters of liquid hydrogen, resulted in an energy loss in the proton beam of 11, 16, and 3 Mev, respectively, as obtained from the range energy curves. Since the neutral meson yield from carbon as a function of the proton energy is given by Crandall, the percentage decrease in meson yield from that at 340 Mev could be obtained. The values chosen were 26 percent for carbon and 41 percent for liquid nitrogen. The correction for hydrogen is uncertain. By referring to the excitation function obtained by Schulz for the $(\rho, \rho\pi^+)$ process, a 5 percent reduction in meson yield would be expected.

When gamma rays pass through matter, their intensity decreases owing to absorption or scattering. Since the energy of the neutral meson decay gamma rays is approximately 70 Mev, the disappearance of the gamma rays will be due to pair production. Knowing the mean free path for pair production for a given material, it is then possible to estimate the percentage decrease in the gamma ray intensity. For the thicknesses of carbon and liquid nitrogen as previously given, the gamma-ray intensity will decrease 4.5 and 8 percent respectively. The liquid hydrogen gives a very small contribution (less than 0.5 percent).

The foregoing corrections were applied to the experimental data and Table II lists the corrected experimental values for proton energies of 340 Mev.

The values obtained for the neutral meson yield from carbon and liquid hydrogen at 90° to the proton beam are listed in Table II. The neutral meson cross section for hydrogen relative to carbon is

$$\sigma_H/\sigma_C = 0.0059 \pm 0.0009.$$

The experimental corrected ratio of the counting rate from liquid nitrogen relative to carbon offers a further check of the consistency of the results as

$$N(\gamma)_N/N(\gamma)_C = 0.546 \pm 0.037.$$

Taking into account of the difference in density of carbon and liquid nitrogen, and further assuming the neutral meson production from liquid nitrogen to be 7/6 of the carbon yield, the expected ratio of the counting rate from liquid nitrogen relative to carbon is

$$N(\gamma)_N/N(\gamma)_C = 0.537.$$

The agreement between the experimental and estimated values listed in Table II give additional evidence that neutral meson production in light nuclei depends primarily on the number of neutrons in the nucleus.

DISCUSSION

On the basis of the discussion given in the introduction, the cross section at higher proton energies may be estimated by using the present experimental results. Since the charged mesons in the $(\rho, \rho\pi^+)$ process are emitted predominately in p states, the quantity $(r_0/\lambda\!\!\!^{-})^2$ can be estimated giving the fraction of mesons that are emitted in p states with respect to the nucleon, but in s states with respect to the center of mass. By forming

$$(r_0/\lambda\!\!\!^{-}_{22})^2 \sigma_{340}(\rho, \rho\pi^+) = \sigma_{340}(\rho, \rho\pi^0),$$

and a similar expression for the 440-Mev reaction one can solve for $\sigma_{440}(\rho, \rho\pi^0)$ at 440 Mev as

$$\sigma_{440}(\rho, \rho\pi^0) = \left(\frac{\lambda\!\!\!^{-}_{22}}{\lambda\!\!\!^{-}_{75}}\right)^2 \frac{\sigma_{440}(\rho, \rho\pi^+)}{\sigma_{340}(\rho, \rho\pi^+)} \sigma_{340}(\rho, \rho\pi^0),$$

where $\lambda\!\!\!^{-}$ is the wavelength of the meson in the center-of-mass system. To evaluate the above expression, it is necessary to estimate the ratio of the $(\rho, \rho\pi^+)$ cross section at 440 Mev to that at 340 Mev.

The $(\rho, \rho\pi^+)$ data at energies of 380 Mev obtained by Passman and Block[25] indicate a T^2 meson energy dependence, where T is the maximum meson kinetic energy in the center-of-mass system. From the data of Schulz at 340 Mev, partial agreement is obtained with a $T^{3/2}$ dependence. A straight T^2 meson energy dependence yields a value for $\sigma_{440}(\rho, \rho\pi^+)/\sigma_{340}(\rho, \rho\pi^+)$ of 11.5. However, if the data of Passman and Block are extrapolated to proton energies of 440 Mev, then the ratio would be approximately 7.

If the extrapolated value is used, the cross section for the $(\rho, \rho\pi^0)$ process at 440 Mev is estimated to be approximately 0.24×10^{-27} cm^2 using the value for the 340-Mev $(\rho, \rho\pi^0)$ process from the experiment. Only fair agreement is obtained with the Chicago result of $0.45 \pm 0.15 \times 10^{-27}$ cm^2; it is uncertain whether the extrapolation is valid.

TABLE II. Neutral meson yields[a] for various targets at 90° to the 340-Mev proton beam. (All errors are standard deviations.)

Target	Total integrator sweeps	Total counts	Time (min)	Experimental value[b] σ/σ_C	Experimental value[b] $N(\gamma)/N(\gamma)_C$	Estimated value[c] σ/σ_C	Estimated value[c] $N(\gamma)/N(\gamma)$
Carbon	60	382±19	27.5	1.0	1.0	1.0	1.0
Liquid nitrogen	145	392±20	66	1.19±0.08	0.546±0.037	1.17	0.536
No target	625	4±2	265	1.0±0.5	0.0009±0.0003	1.2	0.00086
Liquid hydrogen	1659	47±6.8	570	0.0059±0.0009	0.0033±0.0005	···	···

[a] Yields are given per nuclus. The absolute cross section for neutral meson production by 340-Mev protons on carbon was measured by Crandall (reference 11) to be 1.5×10^{-27} cm^2.
[b] Corrected for energy degradation in target and for gamma-ray conversion in the target material.
[c] Values obtained assuming production of neutral mesons to depend only on the number of neutrons.

[25] S. Passman and M. M. Block, Ph.D. dissertation submitted by S. Passman, Columbia University, 1952 (unpublished).

In conclusion, it is shown (1) that the yield of neutral mesons by protons on protons at 440 Mev can be approximately obtained from the result at 340 Mev by a consideration of the energy dependence of meson production, and (2) that there is some evidence for the breakdown of the approximate selection rule which forbids the emission of s state mesons with final s state nucleons.

It is a pleasure to thank Professor E. M. McMillan for his continued interest in this experiment. I am grateful to Drs. J. Lepore, M. Ruderman, and P. Wolff for discussions of the theoretical aspects of the work. I also wish to express appreciation to Mr. J. Garrison for the loan of his liquid hydrogen target, and to the accelerator technical group under the direction of Mr. W. Stockton and Mr. D. O'Connell for their assistance in the construction of the Čerenkov counter. Thanks are also due to the cyclotron operating crew under Mr. J. Vale for their cooperation in making the bombardments.

PHYSICAL REVIEW VOLUME 92, NUMBER 3 NOVEMBER 1, 1953

Studies of X-Rays from Mu-Mesonic Atoms*

VAL L. FITCH AND JAMES RAINWATER
Department of Physics, Columbia University, New York, New York
(Received July 23, 1953)

A new technique of x-ray spectroscopy of μ-mesonic atoms has been developed. The x-rays are produced when a μ^-meson undergoes transitions between Bohr orbits about nuclei of various Z. The mesons are produced by the Columbia University 164-in. Nevis cyclotron. The x-rays are detected, and their energies are measured to better than 1 percent accuracy (for $Z \geq 22$) using a NaI crystal scintillation spectrometer. The $2p \rightarrow 1s$ transition energies were measured to be 0.35, 0.41, 0.955, 1.55, 1.60, 3.50, 5.80, 6.02, and 6.02 Mev for $Z=13$, 14, 22, 29, 30, 51, 80, 82, and 83. Special attention was paid to the Pb spectrum, and it is believed that an 0.2-Mev fine structure splitting has been observed. This is the expected splitting if the μ^- meson is a spin $\frac{1}{2}$ Dirac "heavy electron" of 210 electron masses, having the expected Dirac magnetic moment and having no strong nonelectromagnetic interaction with nuclear matter.

Since the μ^-meson Bohr orbits are 210 times closer to the nucleus than the equivalent electron orbits, the x-ray energies are quite sensitive to nuclear size for medium and large Z. In the case of Pb, a 1 percent change in nuclear radius gives a 1 percent change in the calculated x-ray energy. Assuming constant proton density inside a spherical nucleus of radius $R_0=r_0A^{\frac{1}{3}}$ and the above properties for the μ meson, we obtain $r_0=1.17$, 1.21, 1.22, and 1.17×10^{-13} cm for $Z=22$, 29, 51, and 82. The significance of these results in relation to other nuclear size measurements is discussed.

INTRODUCTION

WHEN a μ^- meson is slowed to rest in condensed matter through loss of its kinetic energy to electrons, it is captured in Bohr type orbits about a nucleus. Then, by a series of radiative and nonradiative (Auger) transitions, the meson proceeds to its K shell in an elapsed time of roughly 10^{-13} to 10^{-14} sec.[1] Thereafter, two competing mechanisms, natural beta decay and nuclear capture, account for the disappearance of the meson from the K shell. The characteristic decay time has been measured to be 2.1 μ sec. The mean time for nuclear capture has been investigated over a wide range of atomic numbers and has been found[2] to vary as Z^{-4} for low Z materials and saturate near 7×10^{-8} sec for $Z=82$. This is a manifestation of the extremely weak interaction (nonelectromagnetic) of μ mesons with nuclear matter. In comparison, the π^- meson will seldom reach the K shell except in the case of nuclei with low atomic number. Experimental studies of π-mesonic x-rays in light elements have been made[3] for low Z elements to investigate this strong absorption. Previously reported results[4] for μ^- mesons have been of a more qualitative nature than the present work and will not be discussed in detail since they are in rough agreement with the present more definite determinations of the transition energies.

When a μ^- meson is "stopped" in a target material and is captured in a Bohr orbit about a particular nucleus, the initial states are characterized by large quantum numbers n and l in view of the large statistical weight associated with these states. The decrease in n soon reaches the point where $n=l+1$, and subsequent transitions have $\Delta n=\Delta l=-1$. Thus the lower states in the cascade usually possess the largest l value consistent with the given total quantum number n (circular orbits).

* This research was supported by the joint program of the U. S. Office of Naval Research and the U. S. Atomic Energy Commission.

[1] E. Fermi and E. Teller, Phys. Rev. **72**, 399 (1947); see also R. E. Marshak, *Meson Physics* (McGraw-Hill Book Company, Inc., New York, 1952), Chaps. 5 and 6 for a general discussion of matters related to the present papers, and for further references.

[2] Keuffel, Harrison, Godfrey, and Reynolds, Phys. Rev. **87**, 942 (1952); see also J. M. Kennedy, Phys. Rev. **87**, 953 (1952).

[3] Camac, McGuire, Platt, and Schulte, Phys. Rev. **88**, 134 (1952).

[4] W. Y. Chang, Revs. Modern Phys. **21**, 166 (1949); E. P. Hinks, Phys. Rev. **81**, 313 (1951); G. G. Harris and T. J. B. Shanley, Phys. Rev. **89**, 983 (1953); F. D. S. Butement, Phil. Mag. **44**, 208 (1953); see G. R. Burbidge and A. H. de Borde, Phys. Rev. **89**, 189 (1953) for other references.

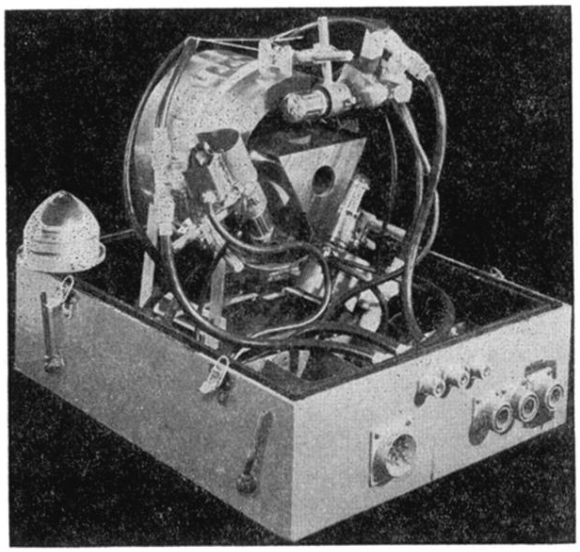

FIG. 3. Photograph of Čerenkov counter.